Plasma Medicine, 1(1): 85–92 (2011)

Plasma-Controlled Cell Migration: Localization of Cold Plasma–Cell Interaction Region

O. Volotskova,[1] A. Shashurin,[1] M. A. Stepp,[2] S. Pal-Ghosh,[2] & M. Keidar[1,*]

[1]School of Engineering and Applied Sciences, Department of Mechanical and Aerospace Engineering, George Washington University, Washington, DC [2]School of Medicine and Health Sciences, George Washington University, Washington, DC

*Address all correspondence to: M. Keidar, George Washington University, School of Engineering and Applied Sciences, Department of Mechanical and Aerospace Engineering, Phillips Hall, Suite 739, 801 22nd Street NW, Washington, DC 20052; keidar@gwu.edu

ABSTRACT: In order to characterize the optimal condition for cell treatment with a plasma jet, its UV-vis-NIR spectrum was evaluated. Furthermore, this study considers the ability of cold atmospheric plasmas to impact cell migration rates as a function of (i) the length of the plasma treatment time, (ii) the number of hours after treatment that cell migration is assessed, and (iii) localization of the treatment zone. Data show that the ability of plasma to reduce cell migration rates increases as a function of treatment time with a maximum of 30%, and that this affect persists for 33 hours after plasma treatment.

KEY WORDS: cold atmospheric plasma, fibroblast cells, migration rates, localization

I. INTRODUCTION

The unique chemical and physical properties of cold atmospheric plasmas enable their numerous recent applications in biomedicine.[1] A wide range of cold plasma applications have been investigated including sterilization, the preparation of polymer materials for medical procedures, wound healing, tissue or cellular removal, and dental drills.[2–7] One of the recent research trends is the investigation of cold atmospheric plasmas' interaction with living tissue at the cellular level.[6–9] Initial experiments on the direct interaction of cold plasmas with living cells demonstrated immediate detachment of treated cells from the extracellular matrix.[2] Later, it was demonstrated that cell detachment occurs for several different cell types including primary mouse fibroblast cells, PAM212 cancer cells, and BEL-7402 liver cancer cells.[5–7] The effects of mild intensity and short duration cold plasma treatment below the threshold required for cell detachment have also been studied.[6,7] It was observed that the migration rate of primary mouse fibroblast cells slowed significantly after mild intensity plasma treatment.[6] Our more recent work[7] was directed at understanding the mechanism by which the plasma jet alters cell migration and induced cell detachment. It was found that integrin expression at the cell surface reduced at plasma treatment. Integrins (transmembrane proteins) are cell adhesion receptors having a dual function, namely, intracellular (integrin occupancy coordinates the assembly of cytoskeletal filaments and signaling complexes) and extracellular (engaging either extracellular

2151-805X/11/$35.00

matrix macromolecules or counter receptors on adjacent cell surfaces). Integrins function in maintaining cell adhesion, tissue integrity, cell migration, and differentiation.[10–12]

Although several recent studies have begun to sort out the cellular and subcellular events altered when cold plasmas interact with living cells, these studies have yet to address the dose response (the relationship between duration of plasma jet interaction with living tissue and a change in the migration rates) and permanency of the migration effects induced in cells by cold plasmas. These types of studies are crucial to allow us to develop safe and practical applications for cold plasmas. Thus, the UV-vis-NIR spectrum of cold plasma jets[13] used in current studies is evaluated. In this paper, we use tertiary-passaged mouse dermal fibroblast cells to show the ability of plasma to reduce cell migration rates, demonstrate the effect of the treatment time, and show the localization of the treatment zone in a single well. Further experiments assess the impact of cold plasma on the pH of the cell culture media immediately after plasma treatment.

II. METHODOLOGY

A. Materials

Wild-type tertiary mouse fibroblast cells were cultured in Dulbecco's modified eagle medium (DMEM) (Invitrogen Corp.) enriched with 5% serum, 1% NEAA, 1% L-glutanine, and 1% Pen-Strep. Diluted cells (30% confluence) were plated in multiwell plates (having a well diameter of about 32 mm) and treated with plasma on the third day in culture. During the experiments, plates with cells were kept on the slide moat (heating plate) (Boekel scientific, model 240000) to maintain the media temperature at 37°C. Trypan blue stain 0.4% (Invitrogen Corp.) was used in "alive-vs-dead" testing.

B. Plasma Jet

The plasma jet operated at 4.5–5 kV, 26–28 KHz, and helium flow rate of about 17 L/min.[6,13] The average discharge power $[(1/T)\int_0^T UIdt$, where U is the output voltage applied to discharge electrodes, I is the discharge current, and T is the period] was ~4.3 W. The plasma jet was targeted to the well center and had a diameter of about 4–5 mm at contact with the well. Cells were kept in the media during the treatment; 2 mL of media per well was used, and the depth of the media was around 2 mm. This amount of media (2 mL per well) was chosen to prevent cell desiccation[6]). The distance between the jet outlet and well surface was around 2 cm. Plasma treatment was conducted with durations from 100 to 500 s (i.e., 430, 860, 1290, 1720, and 2150 J of discharge energy corresponding to 100, 200, 300, 400, and 500 s, respectively). For controlling purposes, cells treated with pure helium for 100 and 300 s (no plasma) and untreated cells were used. The spectrum of the cold atmospheric plasma jet in the air was monitored by means of fibro-optical portable spectrometer (EPP2000 HR Model, StellarNet-Inc) in the UV-vis-NIR range of wavelengths (200–900 nm) with a fibro-optical probe (diameter 1 mm) oriented along and perpendicular to the jet as shown in Figure 1.

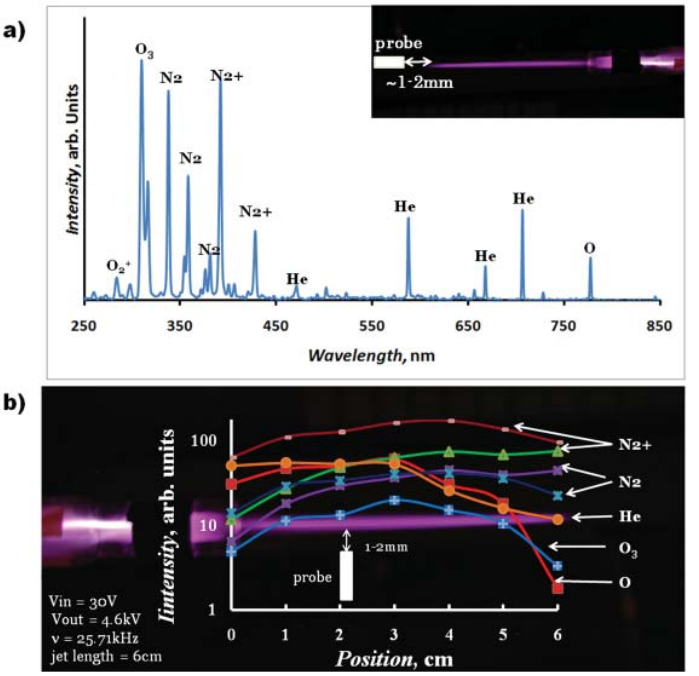

FIGURE 1. (A) UV-vis-NIR spectrum of the jet with assigned elements; schematic of the measurements at the end of jet is shown in the inserted picture. (B) Schematic of the spectroscopic measurements along the jet, and given plasma jet parameters are shown—intensities of O_3, N_2, N_2^+, He, and O are plotted in logarithmic scale.

C. Time-Lapse Studies

Further time-lapse studies were performed on an Olympus IX81 research microscope (Olympus America, Center Valley, Pennsylvania) equipped with a Proscan motorized stage (Prior Scientific Instruments Ltd., Rockland, Massachusettes) and placed in a temperature- and CO_2-controlled chamber (LiveCell Incubation System, Neue Biosciences, Camp Hill, Pennsylvania). Using relief-contrast optics, images (schematic of the axial point distribution is shown in Fig. 2) were taken per well every 10 min for 16 h and 40 min (100 images) and the next 16 h and 40 min to see the dynamics in ~33 h. Images were transferred to a workstation equipped with Metamorph image analysis software (Molecular Devices Corporations, Chicago, Illinois) where velocities of 10 cells were calculated using the track cell module in each tracked location. A more detailed description can be found elsewhere.[14]

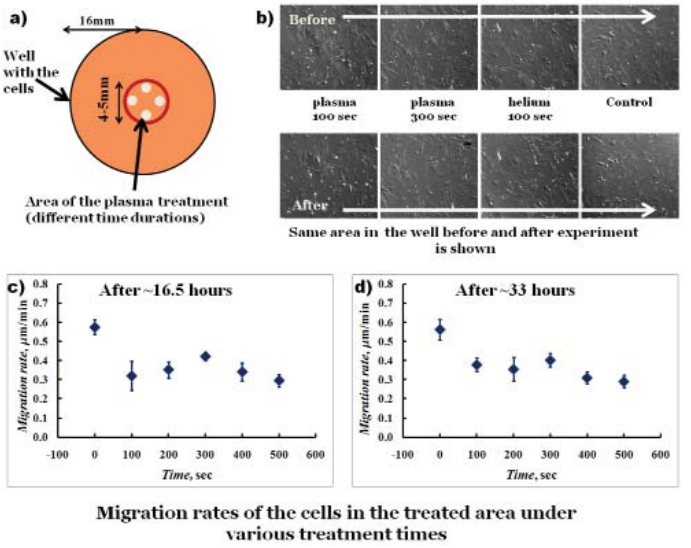

FIGURE 2. (A) Schematic representation of the experiment is shown: reduction in migration rates' dependence on the length of the plasma treatment. Four points were taken inside the treated area and 40 cells analyzed. (B) "Alive-vs-dead" testing of the treated cells with trypan blue stain with the same area in the well analyzed before and after treatment. Cell migration rates for ~0–16.5 h (C) and ~16.5–33 h (D) after treatment as functions of treatment duration. Error bars indicate the standard deviations of data points.

III. RESULTS AND DISCUSSION

Figure 1 shows spectroscopic measurements of the cold atmospheric plasma jet along the plasma jet with given parameters (output voltage ~4.6 kV, frequency ~26 kHz, and helium flow rate ~17 L/min). The assigned spectrum measured at the jet's end is shown in Figure 1A (this spectrum characterizes radiation from the whole length of the plasma column including the discharge inside the Pyrex tube). The presence of atomic helium (He) and oxygen (O) was found in the range 450–900 nm; neutral nitrogen N_2 (second positive system) and N_2^+ (first negative system) degraded to shorter wavelengths; O_2^+ (first negative system, degraded to longer wavelengths) and O_3 (however, its values might be also attributed as a combination of O_2^+ and O^+ species) were identified in the range 200–450 nm.[15] Thus, ionized nitrogen and highly reactive oxygen radicals are presented during the cell treatment. There is no change in the subset of the identified species was found with the increasing of the distance from the nozzle, although there was some variability in the intensities of spectral lines along the jet. The dependences of the intensities of O_3, N_2, N_2^+, He, and O along the plasma jet are shown in Figure 1B

(logarithmic scale). It was observed that the intensity of nitrogen lines increase with distance from the nozzle, while the intensity of He and O_3 decrease. The atomic O does not show significant changes up to 6 cm. Based on these measurements, we can conclude that the optimal condition for maximization of radiation intensity would be 2–3 cm from the nozzle.

Next, we treated cells with cold plasma for times ranging from 100 to 500 s. A schematic diagram indicating how these treatments were made is shown in Figure 2A. Controls included cells treated with helium alone for the same times. Cells were treated with plasma immediately after plasma treatment with trypan blue. We have shown previously that plasma treatments can cause cell death as assessed using trypan blue.[10] Trypan blue is a vital dye that is excluded from entering live cells; dead cells fill with the blue dye. Data shown in Figure 2B for cells treated with plasma or helium alone for the times tested indicate that trypan blue is excluded from cells and, therefore, these treatment times do not cause cell death.

When cell migration is assessed as a function of the duration of plasma treatment, we found in Figure 2C that 100 s significantly reduced cell migration rates when assessed from 0 to 16.5 h after plasma treatment. Treatment times up to 500 s did not further reduce cell migration significantly when assessed between 0 and 16.5 h; however, when migration rates were assessed between 16.5 and 33 h, we again found that 100 s significantly reduced cell migration rates—but also, 500 s of treatment reduced the migration rate even further compared to 100 s. Thus, the general trend becomes: as treatment time increases, the cells migrate slower.

In order to address the effect of plasma treatment on the pH level of DMEM media, we conducted treatments of media at standard experimental conditions described above. One of the components of cell culture media is the acid-base indicator phenol red. At acidic pH, the color of phenol red is yellow; at basic pH, phenol red is pink; and at neutral pH, phenol red is red/orange. These features of phenol red, along with its lack of toxicity, make it an excellent indicator of pH in cell culture media. No change of media color was observed after the 60, 120, and 200 s treatments of media (data not shown), indicating that the pH level of the media remained unchanged at plasma treatment.

In the current study, experiments were performed using tertiary dermal fibroblast cells whereas previously we used primary dermal fibroblasts.[8] This change reduced variability in the cells within each culture and enhanced our ability to obtain statistically significant data. The cell density was carefully controlled by the volume of cells plated and maintaining the cells in culture for three days. It is known that fibronectin fibrils begin to accumulate around cells after three days increasing cell confluence. These fibrils can reduce cell migration rates.

The ability of cold atmospheric plasma treatment to impact cell migration was further considered by evaluating cell migration rates as a function of the distance from the plasma treated zone. A schematic of the experiment is shown in Figure 3A. Three locations of interest were considered, namely, inside the plasma treated area (red circle indicates the treated area, diameter of around 5 mm) and further equidistant at the second and

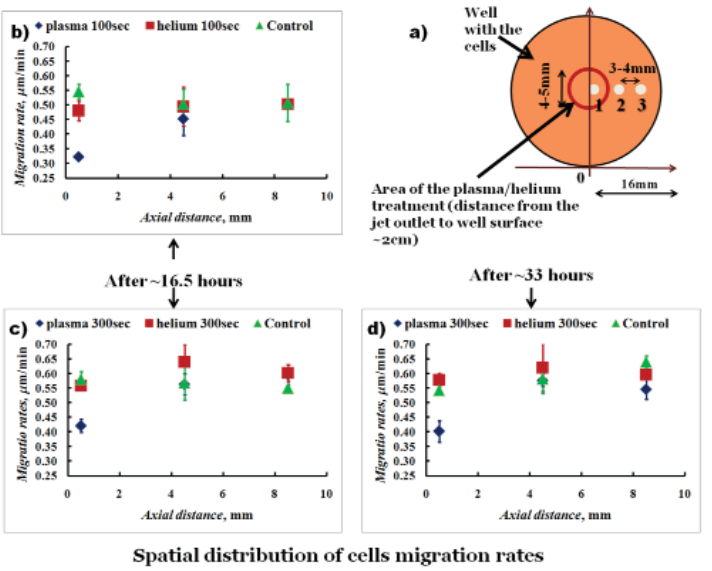

FIGURE 3. (A) The experimental setup for spatial distribution of the cell migration rates for a single well is shown. (B–D) The dependence of cell migration rates versus distance from the center of the treated zone for cells tracked during 0–16.5 h after 100 and 300 s plasma treatment, respectively (B, C), for cells tracked during 16.5–33 h after 300 s plasma treatment (D). Cells treated with plasma, with helium only, and untreated cells are shown. Data is given with standard deviations. The reduction in migration rate is around 30% in the treated area after ~16.5 h (B, C). This trend remains after ~33 h (D) of cell tracking.

third locations outside—each location between two neighbor points was ~3–4mm apart. The average velocity of 10 cells per each tracked location was calculated after 16.5 h. To increase the statistical significance of the results, data were taken symmetrically in six different locations, thus giving 20 cells per point of interest. Experiments were repeated several times with various treatment times of 100 and 300 s. Thus, overall, ~60 cells per each location were analyzed. Figure 3B shows the spatial distribution of migration rates after 100 s of plasma treatment (data shown for 20 cells at each point after 16.5 h of tracking). Neither the only helium or control velocity distributions show any significant changes. However, plasma treated cells showed a localized reduction in their migration rates of around 30–40%. The standard deviation is indicated with vertical bars at the data points; it does not exceed 5%.

Spatial characteristics of the effect on cell migration induced by the plasma treatments are shown in Figures 3B and 3C for cells tracked between 0 and 16.5 h after treatment (cells treated during 100 and 300 s) and in Figure 3D for cells tracked between 16.5 and 33 h after treatment (time duration of treatment 300 s). Again, for controlling

purposes, only helium treated cells and untreated cells are shown. Figures 3B and 3C show that cells treated with plasma (100 s and 300 s) have the slowest migration rates in the treated area (~1 mm from the center of the plate), while cells outside the treated area (5 and 8 mm from the center) migrate at the same rates as untreated cells. Also, no reduction of cell migration was observed in the cells treated with the only helium. It was observed that reduction (around 30%) in cell migration is persistent for 33 h (see Figure 3D).

The reduction of the rates of cell migration can be related to the changes in the integrin expression reported previously by Shashurin et al.[9] It was found that plasma treated cells have a reduction in α_v and β_1 integrins expression, whose functions are related to cell motility and cell adhesions.[8,14] A media bicarbonate buffering system was able to maintain the pH level unchanged,[16] thus, we can conclude that this amount of plasma treatment was not enough to affect it.

IV. CONCLUSIONS

It was shown that the reduction in cell migration under cold plasma treatment is confined to within 5 mm of the treatment zone, which is comparable with the diameter of the plasma jet (4–5 mm). The reduction in cell migration after plasma treatment is shown to be around 30%, which is in the agreement with previous data.[6] This change in cell migration has not only spatial effects, but also temporal, i.e., localization in the migration rate persists at least for 33 h after treatment. The tertiary fibroblast cells used in these experiments provided more statistically reliable data.

REFERENCES

1. Fridman A. Plasma chemistry. New York: Cambridge University Press; 2008.
2. Fridman G, Friedman G, Gutsol A, Shekhter AB, Vasilets VN, Fridman A. Plasma Process Polym. 2008;5:503-533.
3. Stoffels E, Sakiyama Y, Graves DB. IEEE Trans Plasma Sci. 2008;36(4):1441
4. Laroussi M. IEEE Trans Plasma Sci. 2008;36:1612-1614.
5. Lu X, Cao Y, Yang P, Xiong Q, Xiong Z, Xian Y, Pan Y. IEEE Trans Plasma Sci. 2009;37:668.
6. Stoffels E, Kieft IE, Sladek REJ, Van den Bedem LJM, Van der Laan EP, Steinbuch M. Plasma Sources Sci Technol. 2006;15:S169.
7. Zhang X, Li M, Zhou R, Feng K, Yang S. Appl Phys. Lett. 2008;92:021502.
8. Shashurin A, Keidar M, Bronnikov S, Jurjus RA, Stepp MA. Appl Phys Lett. 2008;93 :181501.
9. Shashurin A, Stepp MA, Hawley TS, Pal-Ghosh S, Brieda L, Bronnikov S, Jurjus RA, Keidar M. Plasma Process Polym. 2010;7:294–300.
10. Hynes RO. Integrins: a family of cell surface receptors. Cell. 1987;48:549-554.
11. Bokel C, Brown Integrins in development: moving on, responding to, and sticking to the extracellular matrix. NH. Dev Cell. 2002;3:311–321.

12. Humphries JD, Byron A, Humphries MJ. Integrin ligands at a glance. J Cell Sci. 2006;119(19):3901-3903.
13. Shashurin A, Shneider MN, Dogariu A, Miles RB, Keidar M. Temporary-resolved measurement of electron density in small atmospheric plasmas. Appl Phys Lett. 2010;96 :171502.
14. Jurjus RA, Liu Y, Pal-Ghosh S, Tadvalkar G, Stepp MA. Primary dermal fibroblasts derived from sdc-1 deficient mice migrate faster and have altered αv integrin function. Wound Rep Reg. 2008;16:649–60.
15. Pearse WB, Gaydon AG. The identification of molecular spectra, Hoboken, NJ: Wiley; 1976.
16. Eagle H. Amino acid metabolism in mammalian cell cultures. Science. 1971;174(4008):500–503.